PERGAMON

Available online at www.sciencedirect.com

SCIENCE DIRECT®

Polyhedron 22 (2003) 795–801

POLYHEDRON

www.elsevier.com/locate/poly

Self-assembled xanthate-transition metal polyether macrocycles and cryptands

Paul D. Beer [a,*], Andrew R. Cowley [b], John C. Jeffery [c], Rowena L. Paul [a], Wallace W.H. Wong [a]

[a] *Department of Chemistry, Inorganic Chemistry Laboratory, University of Oxford, South Parks Road, Oxford, OX1 3QR, UK*
[b] *Chemical Crystallography Laboratory, 9 Parks Road, Oxford, OX1 3PD, UK*
[c] *School of Chemistry, University of Bristol, Cantock's Close, Bristol, BS8 1TS, UK*

Received 6 August 2002; accepted 9 October 2002

Abstract

The synthesis of novel dinuclear nickel(II)–xanthate polyether macrocycles and dinuclear cobalt(III)–xanthate polyether cryptands is reported. The assemblies have been characterised by a range of spectroscopic techniques and in one case by X-ray crystal structure determination. Electrospray mass spectrometry provided evidence that the dinuclear nickel(II)–xanthate macrocycles form adducts with Group I metal cations and methyl viologen (MV^{2+}). The dinuclear cobalt(III)–xanthate cryptands also form adducts with Group I metal cations but did not interact with MV^{2+}.

Keywords: Cryptands; Polyether macrocycles; Xanthate; Methyl viologen

1. Introduction

The synthesis of two- and three-dimensional macrocyclic and cage-like host molecules using metal directed self-assembly is a current area of intense research activity [1]. Through prudent choice of metal ion and multidentate ligand components, the resulting self-assembled polymetallic structures can be designed to exhibit unique electronic and magnetic properties, and have the potential to bind guest substrates [1,2]. Presently the field is dominated by square planar platinum(II) metals in combination with various oligopyridine ligands, [1c,3] copper(I), nickel(II), silver(I), iron(II) helical structures of oligobipyridyls [3] and pseudo-octahedral titanium(IV), aluminium(III), iron(III), gallium(III) complexes of oligocatecholate ligands leading to triple helicates [3] and tetrahedral clusters [4]. Using the dithiocarbamate ligand as a self-assembling structural motif for the first time, we have recently synthesised novel nano-sized resorcarene-based transition metal polymetallic assemblies [5] which bind C_{60} [6] and copper(II)–dithiocarbamate macrocycles capable of selectively sensing anionic guest species using electrochemical techniques [7]. This paper describes the synthesis of novel dinuclear macrocycles and cryptands based on metal–xanthate ligand interactions. The coordination chemistry of the xanthate (dithiocarbonate) ligand is well established, [8] however, to our knowledge this ligand has not been exploited in the field of metal directed self-assembly. We report here the incorporation of the xanthate ligand into various polyether linkages, and by using metal directed self-assembly, the synthesis of new dinuclear nickel(II)–xanthate polyether macrocycles and dinuclear cobalt(III)–xanthate polyether cryptands.

2. Results and discussion

2.1. Syntheses

The polyether bis-xanthate salts were prepared in almost quantitative yields via reaction of the appro-

* Corresponding author. Tel.: +44-1865-272632; fax: +44-1865-272690.
E-mail address: paul.beer@chem.ox.uk (P.D. Beer).

0277-5387/03/$ - see front matter © 2003 Elsevier Science Ltd. All rights reserved.
doi:10.1016/S0277-5387(02)01412-2

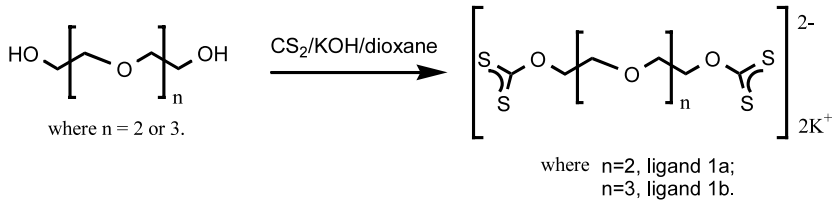

Scheme 1. Synthesis of the polyether xanthate ligands.

priate polyether diol with just over two equivalents of carbon disulfide and KOH base in dioxane solution (Scheme 1). Simply mixing the polyether bis-xanthate salts with aqueous solutions of nickel(II) acetate or cobalt(II) chloride afforded the dinuclear transition metal cyclic products (Schemes 2 and 3). Column chromatography on silica using dichloromethane as eluent purified the respective dinuclear compounds. The dinuclear nickel(II) macrocycles (**2a**) and (**2b**) were isolated in 35 and 37% respective yields, whilst the cobalt (III) cryptands (**3a**) and (**3b**) were obtained as green powders in yields of 34 and 26%, respectively.

The dinuclear assemblies (**2**) and (**3**) were characterised by a variety of techniques including ^{1}H NMR, ^{13}C NMR, UV–Vis spectroscopy and elemental analysis (Section 4). The UV–Vis data obtained for the dinuclear nickel(II) macrocycles (**2a** and **2b**) were comparable to literature values of the mononuclear nickel(II) bis(ethylxanthate) (Table 1). The UV–Vis values for the cobalt(III) cryptands (**3a** and **3b**) were also similar to literature values of the mononuclear cobalt(III) tris(ethylxanthate) (Table 1).

2.2. X-ray structural investigations of potassium polyether xanthate (*1c*) and macrocycle (*2b*)

Crystals of the mono-xanthate polyether potassium salt (**1c**) suitable for structural determination were grown from a solvent mixture of the bis-xanthate polyether potassium salt (**1b**) in acetone, suggesting its presence as a minor contaminant. The structure (Fig. 1) consists of one molecule of (**1c**) encircling a potassium ion with $K^{+}\cdots O$ distances in the range 2.721(1)–3.178(1) Å. The K(1)–S(1) distance is 3.430(1) Å. There are additional interactions with neighbouring molecules giving rise to K–O bond lengths of 2.861(1) Å and K–S bond lengths of 3.351(1) Å. These link the complexes to form chains. Although it would be more desirable to show the crystal structures of the dixanthate polyether salts (**1a** and **1b**), the crystal structure of (**1c**) shows a pre-organisation of the ligand by the potassium cation which may have a role in templating the formation of the dinuclear nickel(II) macrocycles (**2a** and **2b**) and the dinuclear cobalt(III) cryptands (**3a** and **3b**).

Crystals of (**2b**) were obtained by slow evaporation of a dichloromethane solution and the crystal structure of the macrocycle is shown in Fig. 2. The individual bond distances and angles within the molecule are unremarkable and the NiS_4 coordination sphere is essentially planar. The molecule lies on a centre of inversion. The Ni–S contacts are in the range 3.627–4.625 Å and suggest no bonding interaction is occurring. It is interesting to note that no alkali metal cation was bound in the macrocycle as it was the case with the mono-xanthate polyether salt (**1c**).

2.3. Investigation of cation guest binding by dinuclear nickel(II) macrocycles and cobalt(III) cryptands

2.3.1. Group I metal cations

The polyether linkages of macrocycles (**2a** and **2b**) and cryptands (**3a** and **3b**) have the potential to cooperatively bind cationic guest species such as Group I metal cations in an analogous fashion to crown ethers and cryptands.

Electrospray mass spectrometry (ESMS) was used to investigate the Group I coordination chemical properties of the macrocycles and cryptands. Equimolar amounts of Na^{+}, K^{+}, Rb^{+} and Cs^{+} perchlorate salts (1×10^{-4} M) and macrocycle (**2a**) (1×10^{-4} M) in a 1:1

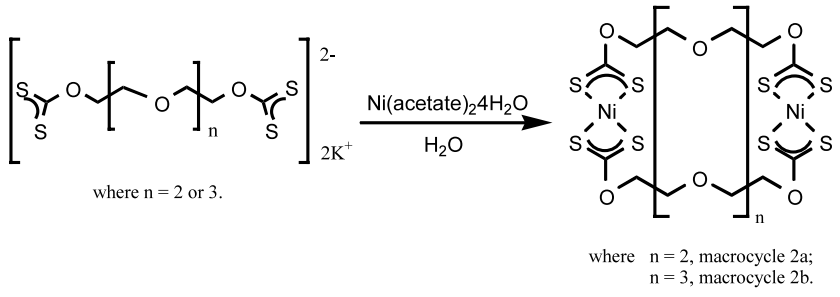

Scheme 2. Formation of dinuclear nickel(II)–xanthate macrocycles (**2a**) and (**2b**).

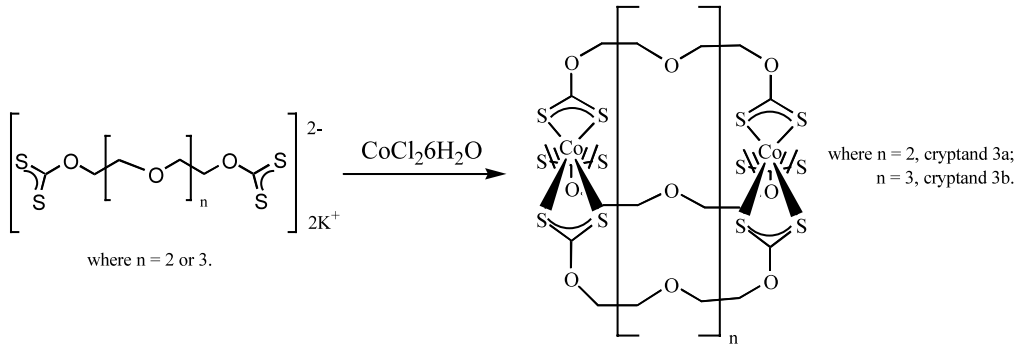

Scheme 3. Synthesis of cobalt(III)–xanthate cryptands (**3a**) and (**3b**).

Table 1
Table of UV–Vis data obtained in CH_2Cl_2

	Wavelength (nm)	ε ($\times 10^3$ M^{-1} cm^{-1})
2a	250	25
	316(316)[a]	45 (25)[a]
	424	4.3
	485(478)[a]	3.0 (2.7)[a]
2b	256	39
	316	67
	423	7.5
	486	5.0
3a	287(285)[b]	39 (32)[b]
	360(353)[b]	11 (13)[b]
3b	287	35
	360	9.4

[a] Literature value for nickel(II) bis(ethylxanthate) measured in chloroform solution [9].
[b] Literature value for cobalt(III) tris(ethylxanthate) measured in chloroform solution [9].

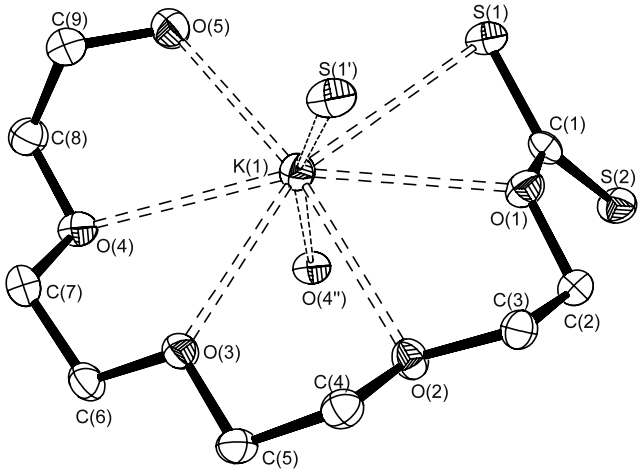

Fig. 1. Thermal ellipsoid plot showing the molecular structure of the mono-xanthate anion and coordination environment of the K^+ cation of compound (**1c**). Thermal ellipsoids are drawn at the 50% probability level. The atoms S(1′) and O(4″) are related to the asymmetric unit by the symmetry operators $2-x$, $1-y$, $1-z$ and $1-x$, $1-y$, $1-z$, respectively. The distances of the coordinating atoms from the K^+ cation are: K1–S1 3.4299(5) Å, K1–S1′ 3.3508(5) Å, K1–O1 2.9163(11) Å, K1–O2 2.9416(11) Å, K1–O3 2.8343(11) Å, K1–O4 3.1783(12) Å, K1–O4 2.8609(11) Å, K1–O5 2.7209(13) Å.

CH_2Cl_2/CH_3CN solvent mixture were added together. The resulting ESMS spectrum (Fig. 3) revealed (**2a**) formed 1:1 adducts with all the alkali metal cations with the signals for Rb^+ and Cs^+ being more intense. Analogous ESMS competition experiments with the larger macrocycle (**2b**) gave similar results, although all $(\mathbf{2b}+M)^+$ adducts were of the same intensity. ESMS competition experiments with Group I metal cations were also performed on cryptands (**3a**) and (**3b**). Equimolar amounts of Na^+, K^+, Rb^+ and Cs^+ perchlorate salts (1×10^{-4} M) in a 1:1 CH_2Cl_2/CH_3CN solvent mixture and cryptand (**3b**) (1×10^{-4} M) in DMSO gave an ESMS spectrum revealing (**3b**) formed 1:1 adducts with all the alkali metal cations with the signals for K^+, Rb^+ and Cs^+ being more intense. No adducts with any alkali metal cations were observed, however, in analogous ESMS competition experiments with the smaller cryptand (**3a**).

UV–Vis spectroscopy Group I metal cation titration experiments in CH_2Cl_2/CH_3CN solutions disappointingly displayed no significant perturbations of the electronic spectra of any of the nickel(II) xanthate macrocycles or cobalt(III) xanthate cryptands. The combination of solubility problems and the broadness of the ^1H NMR spectra of especially (**3a**) and (**3b**) prevented ^1H NMR Group I metal cation titrations being undertaken.

2.3.2. *Methyl viologen binding studies*

The resemblance of the dinuclear nickel(II)–xanthate polyether macrocycle (**2b**) to bis-paraphenylene-34-crown-10 (Fig. 4), prompted an investigation into whether these nickel(II)–xanthate macrocycles formed complexes with the dication, methyl viologen (MV^{2+}), which is known to strongly associate with the aforementioned crown ether in organic solutions via π–π stacking and hydrogen bonding interactions [10]. ESMS examination of equimolar mixtures of (**2a**) or (**2b**) and (MV^{2+}) in 1:1 CH_2Cl_2/CH_3CN solution revealed sig-

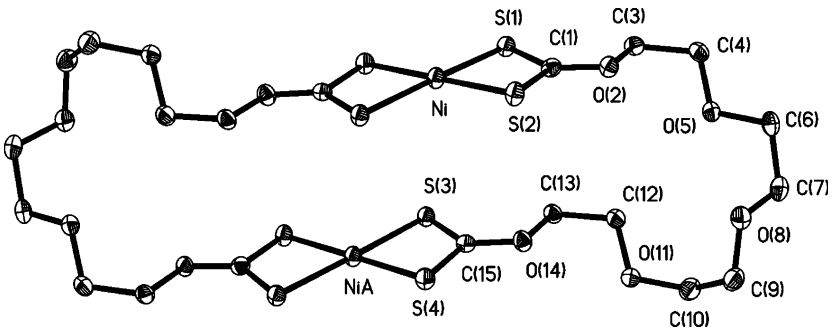

Fig. 2. Thermal ellipsoid plot showing the molecular structure of dinuclear nickel(II)–xanthate macrocycle (**2b**). Formula $C_{20}H_{32}N_{12}O_{10}S_8$, Space group $P\bar{1}$. Selected bond distances: Ni–S(1) 2.2165(6) Å, Ni–S(2) 2.2251(7) Å, NiA–S(3) 2.2285(6) Å, NiA–S(4) 2.2098(7) Å, S(1)–C(1) 1.703(2) Å, S(2)–C(1) 1.697(2) Å, S(3)–C(15) 1.692(2) Å, S(4)–C(15) 1.693(2) Å. Thermal ellipsoids are drawn at the 40% probability level.

nificant $[(\mathbf{2})+(MV^{2+})+(PF_6^-)]^+$ adducts with both macrocycles suggesting complex formation. Subsequent UV–Vis and ^{1}H NMR titrations in 1:1 CH_2Cl_2/CH_3CN with both (**2a**) and (**2b**) however, revealed only very small changes in the respective electronic and NMR spectra indicating interactions between MV^{2+} and the metal macrocycles must be weak.

Interactions of cobalt(III) cryptands (**3a**) and (**3b**) with (MV^{2+}) were also investigated with ESMS experiments. No adducts were observed when equimolar mixtures of (**3a**) or (**3b**) and (MV^{2+}) in DMSO/CH_3CN solution were examined by ESMS.

3. Conclusion

The synthesis of novel dinuclear nickel(II)–xanthate polyether macrocycles and dinuclear cobalt(III)–xanthate polyether cryptands has been achieved via metal directed self-assembly. The assemblies have been characterised by ^{1}H NMR, ^{13}C NMR, UV–Vis spectroscopy, mass spectrometry and elemental analysis, including the X-ray crystal structure determination of a dinuclear nickel(II)–xanthate macrocycle. ESMS provided evidence that the dinuclear nickel(II)–xanthate macrocycles form adducts with Group I metal cations

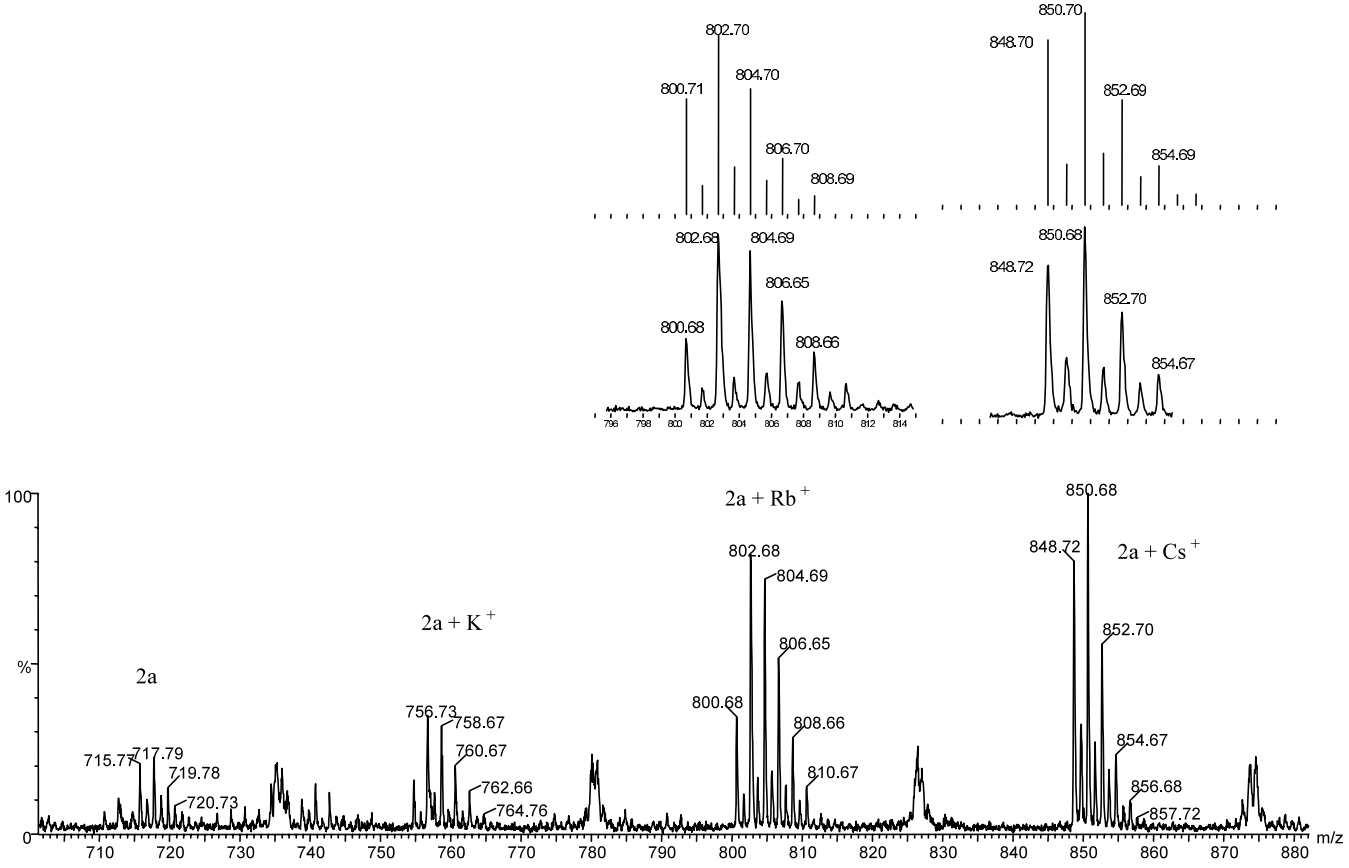

Fig. 3. Positive ESMS of adducts of K^+, Rb^+ and Cs^+ with macrocycle (**2a**).

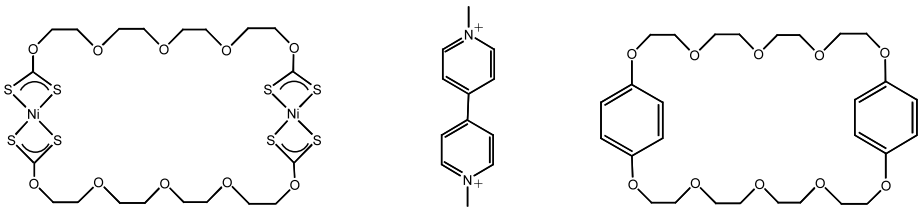

Fig. 4. Resemblance of dinuclear nickel(II)–xanthate (**2b**) with bisparaphenylene-34-crown-10.

and MV^{2+} in organic solutions. Although the cobalt(III)–xanthate cryptands also form adducts with Group I metal cations, no evidence of interaction with MV^{2+} was observed by ESMS.

4. Experimental

4.1. General details

NMR spectra were recorded on a Varian 300 MHz spectrometer. Mass spectrometry was carried out on a Micromass LCT ESMS (cone voltage = 20–50 V, desolvation temperature = 80 °C, source temperature = 60 °C). Elemental analysis was performed at the Inorganic Chemistry Laboratory, Oxford. Electronic spectra were recorded on a Perkin-Elmer Lambda 6 UV–Vis spectrometer.

4.2. Syntheses

4.2.1. Dixanthate polyether salts (*1a*) and (*1b*) and mono-xanthate polyether salt (*1c*)

The procedure for the synthesis of the above polyether dixanthate salts is obtained from Ref. [11]. To a suspension of finely powdered potassium hydroxide (1.1 g, 0.02 mol) in dioxane (20 ml) was added a solution of diol (triethylene or tetraethylene glycol, 0.01 mol) and carbon disulfide (1.8 g, 0.024 mol) in dioxane (10 ml). The mixture was stirred overnight at room temperature. Diethyl ether (7 ml) was added and the mixture was stirred for an additional hour. The pale-yellow solid was collected, washed with ether, and thoroughly dried under vacuum in a dessicator. The salts were obtained in quantitative yield and used as starting materials without further purification. Mono-xanthate polyether salt (**1c**) was also obtained as a trace by-product from the synthesis of the dixanthate salt from tetraethylene glycol as identified by the crystal structure solved for (**1c**).

1a: ^{1}H NMR (300 MHz, D_2O, 294 K) δ (ppm) = 4.41 (m, 4H, S_2COCH_2–), 3.71 (m, 4H, $S_2COCH_2CH_2O$–) and 3.60 (s, 4H, $–OCH_2CH_2O–$). ^{13}C NMR (300 MHz, D_2O, 294 K) δ (ppm) = 232.1 ($–CS_2$), 72.6, 70.0, 69.1, 66.9 and 60.7. ESMS (negative ion, MeOH): *m*/*z* 339 $[C_8H_{12}O_4S_4K]^-$.

1b: ^{1}H NMR (300 MHz, D_2O, 294 K) δ (ppm) = 4.42 (m, 4H, S_2COCH_2–), 3.72 (m, 4H, $S_2COCH_2CH_2O$–), 3.59 (s, 4H, $–OCH_2CH_2O–$) and 3.49 (s, 4H, $–OCH_2CH_2O–$). ^{13}C NMR (300 MHz, D_2O, 294 K) δ (ppm) = 232.1 ($–CS_2$), 72.5, 72.0, 69.9 and 60.7. ESMS (negative ion, MeOH): *m*/*z* 383 $[C_{10}H_{16}O_4S_4K]^-$.

4.2.2. Macrocycles (*2a*) and (*2b*)

An aqueous solution of the dipotassium polyether dixanthate salt (**1a**: 0.38 g, 1 mmol; **1b**: 0.42 g, 1 mmol) was added to an aqueous solution of the nickel(II) acetate tetrahydrate (0.25 g, 1 mmol). The mixture was stirred for 2 h and the precipitate was collected. The green solid was dissolved in CH_2Cl_2 and purified by column chromatography (silica, eluent: CH_2Cl_2/EtOH 9:1). Percentage yield for **2a** = 0.25 g, 35%; **2b** = 0.3 g, 37%.

2a: ^{1}H NMR (300 MHz, $CDCl_3$, 294 K) δ (ppm) = 4.65 (m, 8H, $–S_2COCH_2–$), 3.87 (m, 8H, $S_2COCH_2CH_2O$–) and 3.71 (s, 8H, $–OCH_2CH_2O–$). ^{13}C NMR (300 MHz, $CDCl_3$, 294 K) δ (ppm) = 230.9, 71.3, 71.2 and 68.2. ESMS (positive ion, CH_2Cl_2/MeCN): *m*/*z* 717 (M^+). *Anal.* Calc. for $C_{16}H_{24}O_8S_8Ni_2$: C, 26.76; H, 3.35. Found: C, 27.35; H, 4.22.

2b: ^{1}H NMR (300 MHz, $CDCl_3$, 294 K) δ (ppm) = 4.67 (m, 8H, $–S_2COCH_2–$), 3.92 (m, 8H, $S_2COCH_2CH_2O$–) and 3.70 (m, 16H, $–OCH_2CH_2O–$). ^{13}C NMR (300 MHz, $CDCl_3$, 294 K) δ (ppm) = 230.6, 72.5, 70.9, 68.0 and 61.8. ESMS (positive ion, CH_2Cl_2/MeCN): *m*/*z* 828 (parent + Na^+) and 844 (parent + K^+). *Anal.* Calc. for $C_{20}H_{32}O_{10}S_8Ni_2$: C, 29.79; H, 4.00. Found: C, 29.81; H, 4.02.

4.2.3. Cryptands (*3a*) and (*3b*)

An aqueous solution of the dipotassium polyether dixanthate salt (**1a**: 0.5 g, 1.3 mmol; **1b**: 0.55 g, 1.3 mmol) was added to an aqueous solution of the cobalt(II) chloride hexahydrate (0.21 g, 0.9 mmol.). The mixture was stirred for 2 h and the precipitate was collected. Percentage yield for **3a** = 0.35 g, 34%; **3b** = 0.30 g, 26%.

3a: ^{1}H NMR (300 MHz, d$_6$DMSO, 294 K) δ (ppm) = 4.60 (br, 12H, –S_2COCH_2–), 3.73 (br, 12H, $S_2COCH_2CH_2O$–) and 3.50 (br, 12H, –OCH_2CH_2O–). ^{13}C NMR (300 MHz, d$_6$DMSO, 294 K) δ (ppm) = 222.1, 72.1, 69.6 and 60.0. ESMS (positive ion, MeOH): *m/z* 1057 [parent+K]$^+$, 1163 [parent+PF_6]$^+$, 1202 [parent+KPF_6]$^+$. *Anal.* Calc. for $C_{24}H_{36}O_{12}S_{12}Co_2\cdot 8H_2O$: C, 24.78; H, 4.48. Found: C, 24.80; H, 4.35.

3b: ^{1}H NMR (300 MHz, d$_6$DMSO, 294 K) δ (ppm) = 4.66 (br, 12H, –S_2COCH_2–), 3.77 (br, 12H, $S_2COCH_2CH_2O$–) and 3.54 (br, 24H, –OCH_2CH_2O–). ^{13}C NMR (300 MHz, d$_6$DMSO, 294 K) δ (ppm) = 223.1, 73.2, 70.9, 69.5 and 61.1. ESMS (positive ion, MeOH): *m/z* 1188 [parent+K]$^+$ and 1371 [parent+KPF_6+K]$^+$. *Anal.* Calc. for $C_{30}H_{48}O_{15}S_{12}Co_2\cdot 5H_2O$: C, 29.06; H, 4.68. Found: C, 29.20; H, 4.44.

4.3. X-ray crystallography

Details of the crystal, data collection and refinement parameters for the new structures are summarised in Table 2. Data for (**1c**) was collected at 150 K in an Enras-Nonius KappaCCD diffractometer using graphite monochromatised Mo Kα radiation ($\lambda = 0.71073$ Å). Intensity data were processed using the DENZO-SMN package [12]. The structure was solved by direct methods using the SIR-92 program [13]. Full-matrix least-squares refinement was carried out using the CRYSTALS program suite [14]. The hydroxyl H atom was located in a difference Fourier map and its coordinates and isotropic thermal parameters subsequently refined. All other hydrogen atoms were positioned geometrically after each cycle of refinement. A Chebychev polynomial weighting scheme was applied.

Data for (**2b**) was collected at 100 K in a Bruker Proteum diffractometer with a 6 kW Cu rotating anode and Osmic beam focus using graphite monochromatised Cu Kα radiation ($\lambda = 1.54184$ Å). Three sets of low angle data and three sets of high angle data were collected to give a sphere of data consisting of a total of 3600 frames of data. A weighting scheme of the form $w = 1/[\sigma^2(F_o^2)+(0.0427P)^2+0.3298P]$ where $P = (F_o^2+2F_c^2)/3$ was applied. Structure solution and refinement used the SHELX package (version 5.03) comprising SHELXS-97 [15] and SHELXL-97 [16]; absorption corrections were applied to the data using SADABS [17]. H atoms were included in calculated positions with isotropic thermal parameters and refined as riding atoms.

Table 2
Table of crystallographic data for compounds **(1c)** and **(2b)**

	Compound **1c**	Compound **2b**
Empirical formula	$C_9H_{17}K_1O_5S_2$	$C_{20}H_{32}Ni_2O_{10}S_8$
Formula weight	308.45	806.36
Temperature (K)	150(2)	100 (2)
Radiation λ (Å)	0.71073	1.54178
Space group	$P2_1/c$	$P\bar{1}$
Crystal system	monoclinic	triclinic
Unit cell dimensions		
a (Å)	9.0960(2)	7.9203 (12)
b (Å)	11.6098(2)	8.6275 (13)
c (Å)	13.7625(3)	11.7324 (18)
α (°)		78.502 (7)
β (°)	104.5053(7)	86.014 (7)
γ (°)		80.330 (6)
V (Å^3)	1407.0	773.9 (2)
Z	4	1
Density (calculated) Mg m^{-3}	1.4556	1.730
Absorption coefficient (mm^{-1})	0.680	6.995
$F(0\ 0\ 0)$	649.782	416
Crystal size (mm)	0.12 × 0.12 × 0.24	0.10 × 0.10 × 0.06
Crystal colour/shape	pale yellow/ fragment	green/block
θ Range for data collection (°)	5–28	3.85–67.09
Index ranges	$-11 \leqslant h \leqslant 11$, $0 \leqslant k \leqslant 15$, $0 \leqslant l \leqslant 17$	$-9 \leqslant h \leqslant 8$, $-9 \leqslant k \leqslant 10$, $-12 \leqslant l \leqslant 13$
Reflections collected/unique	22 187/3381 [$R_{int} = 0.032$]	4929/2419 [$R_{int} = 0.0222$]
Max/min transmission	0.92/0.85	0.6789/0.5414
Data/restraints/parameters	2445/0/158	2228/0/181
Goodness-of-fit on F^2	1.0350	1.055
Final R indices [$I > 2\sigma(I)$]	$R_1 = 0.0251$, $wR_2 = 0.0291$	$R_1 = 0.0276$, $wR_2 = 0.0754$
R indices (all data)	–	$R_1 = 0.0296$, $wR_2 = 0.0769$
Largest difference peak and hole (e Å^{-3})	0.63 and −0.28	0.480 and −0.293

5. Supplementary material

Crystallographic data for the structural analyses have been deposited with the Cambridge Crystallographic Data Centre, CCDC numbers 190 574 for (**1c**) and 190 575 for (**2b**). Copies of this information may be obtained free of charge from The Director, CCDC, 12 Union Road, Cambridge, CB2 1EZ, UK (fax: +44-1223-336033; e-mail: deposit@ccdc.cam.ac.uk or http://www.ccdc.cam.ac.uk).

Acknowledgements

We gratefully acknowledge the Leverhulme Trust for a postdoctoral fellowship (R.L.P) and the EPSRC for a studentship (W.W.H.W).

References

[1] (a) R.W. Saalfrank, B. Demleitner, in: J.P. Sauvage (Ed.), Transition Metals in Supramolecular Chemistry, Perspectives in Supramolecular Chemistry, vol. 5, Wiley, Weinheim, 1999, p. 1;

(b) R.W. Saalfrank, I. Berra, Curr. Opin. Solid State Mater. Sci. 3 (1998) 407;
(c) M. Fujita, Chem. Soc. Rev. 27 (1998) 417;
(d) C.J. Jones, Chem. Soc. Rev. 27 (1998) 289.
[2] S. Leininger, B. Olenyuk, P. Stang, Chem. Rev. 100 (2000) 853.
[3] (a) B. Hasenknopf, J.-M. Lehn, B.O. Kneisel, G. Baum, D. Fenske, Angew. Chem., Int. Ed. Engl. 35 (1996) 1838;
(b) B. Hasenknopf, J.-M. Lehn, N. Bourneďiene, A. Dupont-Gervais, A. Van Dorsselaer, B. Kneisel, D. Fenske, J. Am. Chem. Soc. 119 (1997) 10956.
[4] (a) M. Albrecht, Chem. Soc. Rev. 27 (1998) 281;
(b) D.L. Caulder, K.N. Raymond, J. Chem. Soc., Dalton Trans. (1999) 1185;
(c) T.N. Parac, M. Scherer, K.N. Raymond, Angew. Chem., Int. Ed. Engl. 39 (2000) 1239.
[5] O.D. Fox, M.G.B. Drew, P.D. Beer, Angew. Chem., Int. Ed. Engl. 39 (2000) 135.
[6] O.D. Fox, G.B. Drew, E.J.S. Wilkinson, P.D. Beer, Chem. Commun. (2000) 391.
[7] P.D. Beer, M.G.B. Drew, O.D. Fox, M.E. Padilla-Tosta, S. Patell, Chem. Commun. (2001) 199.
[8] (a) S.R. Rao, Xanthates and Related Compounds, Marcel Dekker, New York, 1971;
(b) E.R.T. Tiekink, G. Winter, Rev. Inorg. Chem. 12 (1992) 183.
[9] C.K. Jorgensen, J. Inorg. Nucl. Chem. 24 (1962) 1571.
[10] B.L. Allwood, N. Spencer, H. Shahriari-Zavareh, J.F. Stoddart, J.D. Williams, J. Chem. Soc., Chem. Commun. 14 (1987) 1064.
[11] N. Fukada, T. Tanaka, T. Fukuya, Y. Takeda, Bull. Chem. Soc. Jap. 70 (10) (1997) 2515.
[12] Z. Otwinowski, W. Minor, Processing of X-ray diffraction data collected in oscillation mode, in: C.W. Carter, R.M. Sweet (Eds.), Methods Enzymol, Academic Press, New York, 1997, p. 276.
[13] A. Altomare, G. Cascarano, G. Giacovazzo, A. Guagliardi, M.C. Burla, G. Ploidori, M. Camalli, J. Appl. Crystallogr. 27 (1994) 435.
[14] D.J. Watkin, C.K. Prout, J.R. Carruthers, P.W. Betteridge, R.I. Cooper, CRYSTALS, Issue 11, Chemical Crystallography Laboratory, Oxford, UK, 2001.
[15] G.M. Sheldrick, SHELXS-97, Program for Automatic Solution of Crystal Structures, University of Göttingen, Göttingen, Germany, 1997.
[16] G.M. Sheldrick, SHELXL-97, A Program for Crystal Structure Refinement, University of Göttingen, Göttingen, Germany, 1997.
[17] G.M. Sheldrick, SADABS: A Program for Absorption Correction of Crystallographic Data, University of Göttingen, Göttingen, Germany, 1997.